

# The Strength Properties of Iron Aluminides

Kyosuke Yoshimi and Shuji Hanada

**Author's Note:** All compositions are provided in mole percent.

*For the development of Fe-Al alloys as structural materials, a deep understanding of slip and deformation properties is necessary. In particular, since mechanical properties of the iron aluminides are affected by excess vacancy strengthening as well as the positive-temperature dependence of yield stress, controlling these strength features is essential. In this article, the strength properties of iron aluminides are reviewed.*

## INTRODUCTION

Iron alloyed with aluminum forms ordered phases based on body-centered cubic (bcc)-derivative superlattices designated as D0<sub>3</sub> and B2 structure over a wide range of aluminum content (23–50 percent).<sup>1</sup> These iron aluminides (i.e., D0<sub>3</sub>Fe<sub>3</sub>Al and B2 FeAl) exhibit a positive temperature dependence of yield stress over the aluminum concentration range, irrespective of the ordering state. This is very attractive for high-temperature structural application.

These aluminides deform by slip below a moderate temperature along the close-packed direction  $\langle 111 \rangle$  on the close-packed plane  $\{110\}$  in the same manner as bcc metals.<sup>2–4</sup> A superdislocation having the Burgers vector of  $a\langle 111 \rangle$  dissociates into a four-fold superlattice dislocation in Fe<sub>3</sub>Al and a

two-fold superlattice dislocation in FeAl to reduce self-energy of the dislocation, where  $a$  is the lattice constant. Dissociated superpartial dislocations having  $b = a/4\langle 111 \rangle$  of Fe<sub>3</sub>Al and  $b = a/2\langle 111 \rangle$  of FeAl are bound with antiphase boundaries (APBs).<sup>2–10</sup> Above the moderate temperature, the slip transition occurs from  $\langle 111 \rangle$  to  $\langle 100 \rangle$ .<sup>11–14</sup> In some B2 aluminides such as NiAl and CoAl,<sup>15–17</sup>  $\langle 100 \rangle$  dislocations are activated instead of  $\langle 111 \rangle$  because their APB energy is high, and, thereby, the dissociation is not energetically preferable. However, it is unlikely that APB energy increases with increasing temperature in Fe-Al. Indeed, the APB energies have been found to decrease at elevated temperatures.<sup>18</sup> The slip transition is governed by the increase in the glide resistance of  $\langle 111 \rangle$  dislocations. Therefore, the detailed knowledge of  $\langle 111 \rangle$  slip is necessary for understanding the strength properties of iron aluminides.

## EXCESS VACANCY STRENGTHENING

Iron aluminides inherently contain a high concentration of thermal vacancies at high temperatures, and the concentration increases with increasing aluminum content.<sup>19–23</sup> Their vacancy-formation enthalpies are 0.9–1.2 eV, which are similar to those of pure metals, whereas their

vacancy-formation entropy is extremely high ( $S = 6k_B$ , where  $k_B$  is the Boltzmann's constant).<sup>24,25</sup> This is the reason why the vacancy concentration in Fe-Al alloys is enormous at high temperatures. Furthermore, iron aluminides have greater vacancy-migration enthalpies of 1.5–1.8 eV.<sup>24,25</sup> Thus, most thermal vacancies are easily retained by rapid cooling. This is in contrast to pure metals, whose formation enthalpy is greater or equal to the migration enthalpy. Consequently, the concentration of excess vacancies exhibits the same aluminum-concentration dependence as that of thermal vacancies.<sup>19,26</sup> Vacancies in B2 FeAl have been reported to be predominantly formed on the iron sublattice, together with an even higher concentration of antisite atoms on either sublattice.<sup>23,27–30</sup> Also, divacancy formation was pointed out due to a relatively high divacancy-binding energy of 0.57 eV.<sup>27</sup>

Excess vacancy strengthening is significant at low temperatures in Fe-Al alloys, particularly in B2 FeAl. Special attention has been paid to this phenomenon since Nagpal and Baker reported the composition and cooling-rate dependence of hardness in B2 FeAl.<sup>31</sup> This phenomenon was first reported by Rieu and Goux.<sup>32</sup> They revealed that B2 FeAl quenched rapidly from elevated temperatures retains a high concentration of thermal vacancies, and retained excess vacancies in B2 FeAl enhance hardness. Since the excess vacancy concentration increases with increasing aluminum content, the strength properties of iron aluminides exhibit strong composition dependence if samples were subjected to the same thermal histories.<sup>19,31,33</sup> In addition, there is a linear relationship between the hardness and the square root of excess vacancy concentration.<sup>19</sup> The increase in hardness leads to the increase in yield stress and critical-resolved shear stress.<sup>34–37</sup>

Figure 1 shows resolved shear stress-shear strain curves of Fe-33 and 44Al single crystals deformed at room temperature in tension.<sup>38</sup> These single crystals were homogenized at 1,373 K for 48 hours and slowly cooled to room temperature at the cooling rate of  $5 \times 10^{-3} \text{ K} \cdot \text{s}^{-1}$  (as-homogenized specimen). After homogenization, the crystals were kept at 1,173 K for one hour and air-cooled to introduce excess vacancies (air-

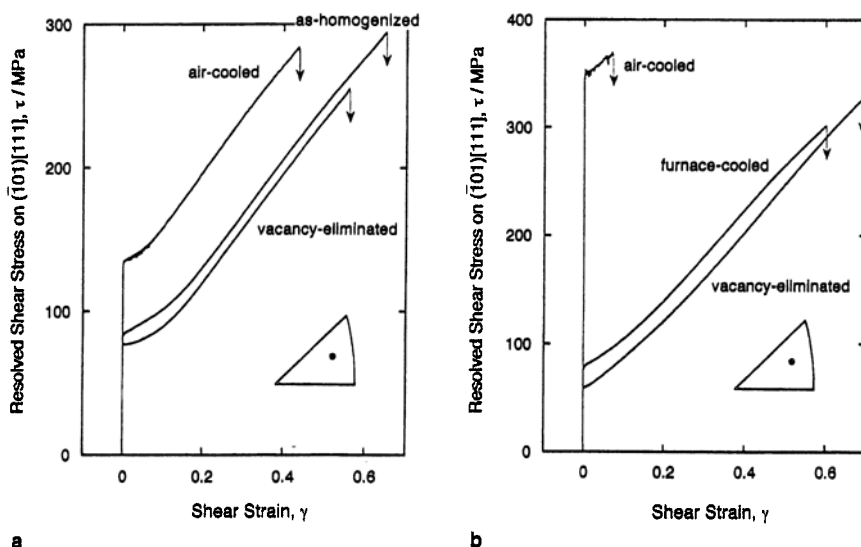


Figure 1. Resolved shear stress-shear strain curves of single crystals in tension at room temperature and an initial strain rate of  $1.6 \times 10^{-4} \text{ s}^{-1}$  (a constant cross-head speed) in a vacuum of better than  $4 \times 10^{-4} \text{ Pa}$  for (a) Fe-33Al and (b) Fe-44Al.

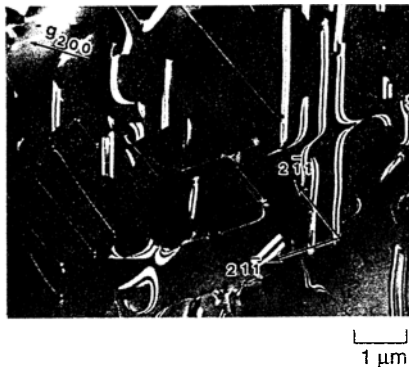


Figure 2. A dark-field electron micrograph taken using the 200 superlattice reflection in  $D0_3$  superlattice.

cooled specimen). Furthermore, the air-cooled specimens were annealed at 698 K for 100 hours to eliminate excess vacancies (vacancy-eliminated specimen). In both alloys, the critical-resolved shear stress is raised, and elongation is reduced by air-cooling. The air-cooled single crystals show Lüders yielding. Slip becomes inhomogeneous by the excess vacancy strengthening.

The effect of cooling rate on hardness was not as marked at aluminum concentrations less than 35%.<sup>31</sup> The results of the single crystals' tensile properties in Figure 1 demonstrate a marked effect of the cooling rate, even for Fe-33Al. On the other hand, the vacancy-eliminated single crystals are relatively ductile. Elongation of more than 30% was observed at room temperature in B2 FeAl single crystal,<sup>39</sup> but, such a large elongation has never been obtained in polycrystals.

### SECONDARY DEFECT STRENGTHENING

While the concentration of retained excess vacancies is reduced by intermediate-temperature annealing,<sup>31,32,40</sup> several types of defect clusters result from the condensation of those vacancies. There are roughly four kinds of secondary extended defects: complex planar fault (CPF) on {100} plane, APB on {111} plane,  $\langle 111 \rangle$  superdislocation, and  $\langle 100 \rangle$  dislocation. CPFs are a planar fault having both APB and stacking fault (SF) character and have been observed only in boron-added Fe-35Al.<sup>41</sup> Unfortunately, the atomistic structure and the formation mechanism of CPFs are not understood. APBs on {111} have been observed in alloys containing 35–42% aluminum.<sup>33,41–43</sup>

Figure 2 shows a typical APB structure in Fe-35Al annealed at 698 K for 120 hours after air-cooling from 1,273 K.<sup>41</sup> All end-on APBs are parallel to the  $[2\bar{1}\bar{1}]$  or  $[2\bar{1}1]$  direction, indicating that these APBs are on  $(1\bar{1}1)$  or  $(11\bar{1})$ . The APB formation is interpreted as a result of the collapse of the lattice owing to vacancy condensation on triple layers of {111} planes during the intermediate-tempera-

ture heat treatment.<sup>41</sup> Such APB formation implies that APB energy is lower on the {111} plane than on other planes. This implication is in good agreement with the result of Flinn's calculation.<sup>5</sup> The size, distribution, and planarity of APBs are affected by alloying elements.<sup>41</sup>

In Fe-40Al<sup>42</sup> and Fe-42Al,<sup>33,43</sup>  $\langle 111 \rangle$  superdislocations have been observed, but CPFs have not. Voids, probably formed by vacancy agglomeration, have been found as well as  $\langle 111 \rangle$  or  $\langle 100 \rangle$  dislocations in Fe-43Al<sup>44</sup> and Fe-45Al-0.1Ni.<sup>45</sup> At near-stoichiometric composition,  $\langle 100 \rangle$  dislocations are predominant.

These observations indicate that the types of defect clusters formed by vacancy condensation are dependent on aluminum concentration as well as heat-treatment histories. The increase in the density of the secondary defects leads to the increase of internal stress. Hence, yield stress is also increased by these factors, but is more sensitive to excess vacancy strengthening than to secondary defect strengthening (Figure 3).<sup>46</sup>

### THIRD ELEMENTS EFFECTS

The fracture mode of polycrystalline Fe-Al alloys is dependent on aluminum concentration. In general,  $Fe_3Al$  and iron-rich FeAl (containing less than 40% aluminum) fracture transgranularly.  $Fe_3Al$  has good ductility by nature and shows elongation of about 12% at room temperature in vacuum, but is embrittled by an external factor (i.e., environmental embrittlement).<sup>47,48</sup> In Fe-Al, cleavage strength is reduced by hydrogen, thereby promoting transgranular fracture. McKamey et al. found that environmental embrittlement is improved to some extent by chromium addition.<sup>49,50</sup>

FeAl containing more than 40% aluminum fractures intergranularly and is less ductile than  $Fe_3Al$ . Also, polycrystalline FeAl is less sensitive to the environmental effect owing to intrinsically weak cohesive strength of grain boundaries.<sup>51</sup> However, FeAl exhibits relatively good ductility at a high strain rate of  $10^{-1}$  to  $10^9$  s<sup>-1</sup> in spite of intergranular fracture,<sup>52</sup> suggesting that polycrystalline FeAl is also embrittled by the environmental effect. Correspondingly, environmental embrittlement in FeAl has been confirmed using single crystals.<sup>53</sup> Also, the increase in the lattice resistance due to the excess vacancy strengthening leads to drastic embrittlement.<sup>34–37</sup> To improve the excess vacancy embrittlement, the effect of third elements (Cu, Ni, Co, Mn, Cr, V, and Ti) on hardening has been investigated.<sup>54,55</sup> Although the addition of the third elements alleviates the excess vacancy strengthening accompanied with solid-solution strengthening, it reduces elongation even if the fracture mode is changed from intergranular to transgranular.<sup>56</sup>

### WORK HARDENING

High work-hardening rates of 1–10 GPa have been reported for iron aluminides.<sup>36,57–60</sup> Ordered alloys generally have a higher work-hardening rate than disordered alloys due to the dislocation-APB interaction.<sup>5,61</sup> Leamy and Kayser<sup>6</sup> schematically described the dislocation-APB interaction process in the  $D0_3$  superlattice and discussed the contribution of antiphase domains to the flow stress of  $Fe_3Al$ . Later, the work hardening of  $Fe_3Al$  was interpreted in terms of APB energies.<sup>7</sup> Based on recent transmission electron microscopy observations, APB blocking<sup>60</sup> and APB tube formation<sup>62</sup> are considered to further enhance the work hardening in Fe-Al. By contrast, excess vacancies reduce the work-hardening rate (Figure 3).

### POSITIVE-TEMPERATURE DEPENDENCE OF YIELD STRESS

Positive-temperature dependences have been observed in several intermetallics since the 1950s. For iron aluminides, it has been well known that  $D0_3$   $Fe_3Al$  has a yield-stress anomaly related to the  $D0_3$ -B2 phase transformation.<sup>63</sup> On the other hand, the yield-stress anomaly of B2 FeAl was not revealed until recently because excess vacancy strengthening obscured the appearance of it.<sup>64</sup>

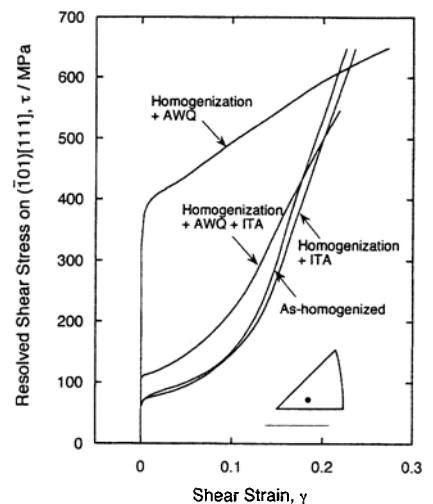


Figure 3. The resolved shear stress-strain curves of Fe-39Al single crystals subjected to four kinds of heat treatment in compression. Homogenization was performed at 1,373 K for 48 hours, followed by slowly cooling to room temperature at the cooling rate of  $5 \times 10^{-3}$  K · s<sup>-1</sup>. Dislocation density after homogenization is about  $10^{12}$  m<sup>-2</sup>. ITA means the intermediate temperature annealing at 698 K for 120 hours followed by furnace-cooling to room temperature at the rate of about  $3 \times 10^{-2}$  K · s<sup>-1</sup>. Dislocation density after homogenization + ITA is about  $10^{12}$  m<sup>-2</sup>. AWQ means the annealing at 1,173 K for 24 hours followed by water-quenching in a silica tube. Dislocation density after homogenization + AWQ + ITA is about  $10^{13}$  m<sup>-2</sup>.

The first sign for the yield-stress anomaly of FeAl was found in Fe-37Al-2Ni in 1987.<sup>65</sup> Later, an anomalous peak was detected in polycrystalline Fe-40Al+B.<sup>66</sup> Also, a distinct peak was observed in large-grained, directionally solidified Fe-40Al.<sup>67</sup>

Since the works of J. Guo et al. and K.-M. Chang,<sup>66,67</sup> this unusual yield behavior has become one of the hottest topics in B2 FeAl. Figure 4 shows the temperature dependence of yield stress of D0<sub>3</sub> Fe-25.8Al<sup>68</sup> and B2 Fe-39.5Al<sup>69</sup> single crystals. As seen, the positive-temperature dependence of yield stress in Fe-Al does not appear at the lower-temperature range, but only appears at the intermediate-temperature range. The yield stresses of Fe-39.5Al exhibit a single peak for all of the orientations examined. In our studies<sup>39,69</sup> the observed onset temperatures ( $T_c$ ) where yield stress begins to increase with increasing temperature lie between  $0.37 T_c$  ( $0.35 T_m$ ) and  $0.44 T_c$  ( $0.41 T_m$ ), and the peak temperatures ( $T_p$ ) lie between  $0.51 T_c$  ( $0.47 T_m$ ) and  $0.59 T_c$  ( $0.55 T_m$ ) near 40% aluminum concentration, where  $T_c$  is the B2/A2 transformation temperature and  $T_m$  the melting point from the phase diagram.<sup>70</sup> The yield stresses of Fe-25.8Al also exhibit a single peak. However, the peak temperatures lie above  $T_c$ , and shoulders appear just below  $T_c$  in the curves for all the orientations examined. This suggests that the yield-stress anomaly is induced not only by the phase transformation but other physical sources.

Peak temperatures in the Fe-Al system that were reported by many researchers<sup>14,18,39,63-69,71-81</sup> are summarized in Figure 5. The yield-stress anomaly can be observed within the entire aluminum-concentration range of the aluminides. At aluminum concentrations less than about 30%, the  $T_p$  data are located around 800 K with a small scatter. The role of

first-order and second-order (D0<sub>3</sub>/B2) phase transformations is certainly recognized as one of the possible causes for the good reproducibility of the peak temperatures at lower aluminum concentrations. However, a few binary data lie above the transformation temperature.<sup>18,68,79</sup> At aluminum concentrations greater than 30%, the observed peak temperatures are much more scattered. These anomalous peaks are not associated with any phase transformation. In studies using single crystals,<sup>69</sup> it was found that  $T_p$  is associated with the slip-transition temperatures. Moreover,  $\langle 111 \rangle$  slip is predominantly activated at the early stage of plastic deformation corresponding to a yield strain even at  $T_p$ , and the slip direction changes to  $\langle 100 \rangle$  during deformation with strain at  $T_p$ .<sup>82</sup>

These results indicate that the yield-stress anomaly is induced by the increase in the glide resistance to  $\langle 111 \rangle$  superdislocations as temperature increases. Therefore, a common strengthening mechanism other than the phase transformations operating on  $\langle 111 \rangle$  superdislocations is expected in the wide composition range, irrespective of the ordered states. Since the yield stress above  $T_p$  is governed by the critical-resolved shear stress of  $\langle 100 \rangle$  slip,  $T_p$  is determined as the intersection between the yield stress versus temperature curves for the  $\langle 111 \rangle$  slip and the  $\langle 100 \rangle$  slip. The yield stresses above  $T_p$  drop quite rapidly, indicating that the decline of glide stress of  $\langle 100 \rangle$  slip is drastic. Accordingly, enhancing the glide resistance for  $\langle 100 \rangle$  slip should be more effective in improving high-temperature strength. For the D0<sub>3</sub>-ordered phase, elevating the D0<sub>3</sub>/B2 transformation temperature also would be available. Titanium and molybdenum additions are effective in modifying the high-temperature strength performance in Fe<sub>3</sub>Al.<sup>83</sup>

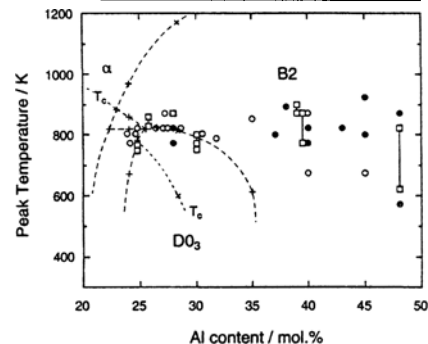


Figure 5. The peak temperature reported in the references as a function of aluminum concentration. — binary single crystals, □ — binary polycrystals, and ● — polycrystals modified by added elements. Broken and dotted lines indicate the phase transformation and the Curie temperature reported.<sup>70,87</sup>

To explain the yield-stress anomaly of Fe-Al, a cross-slip pinning (CSP) model,<sup>18</sup> a local climb locking (LCL) model,<sup>84,85</sup> and a vacancy-strengthening model<sup>86</sup> were presented. In both the CSP and LCL models, energetic preferences due to the anisotropy of APB energy have been pointed out. Recovery becomes active gradually as temperature increases above  $T_p$ , meaning the acceleration of atomic diffusion at the temperature range.<sup>82</sup> In any case, the change in the core structure of  $\langle 111 \rangle$  superdislocation, including the interaction between the dislocation and vacancies, seems to generate pinning force against dislocation motion. A conclusive mechanism of the anomaly has not been established.

## CONCLUSIONS

Excess vacancy strengthening is an intrinsic property in iron aluminides, thereby reducing their ductility, especially in B2 FeAl. No expedient method that alleviates the excess vacancy embrittlement in ductile Fe-Al has been proposed. Also, there has been no plausible interpretation for the excess vacancy strengthening in the iron aluminides. Fe<sub>3</sub>Al is more beneficial than FeAl because of weak excess vacancy strengthening, although the lower density of FeAl is very attractive for structural material applications.

Iron aluminides exhibit positive-temperature dependence of yield stress through the entire aluminum concentration, irrespective of the ordered state. The definite physical source(s) inducing this phenomenon has not been revealed, but the glide resistance for  $\langle 111 \rangle$  slip increases as temperature increases. Thus, enhancing the glide resistance for  $\langle 100 \rangle$  slip should be considered in improving the high-temperature strength of the iron aluminides.

## References

- 1 T B Massalski et al., ed., *Binary Alloy Phase Diagrams*, (Metals Park, OH: ASM, 1986), p 112
- 2 M.J. Marcinkowski and N. Brown, *Acta Metall.* 9 (1961), p 764
- 3 H.J. Leamy, F.X. Kayser, and M.J. Marcinkowski, *Phil*

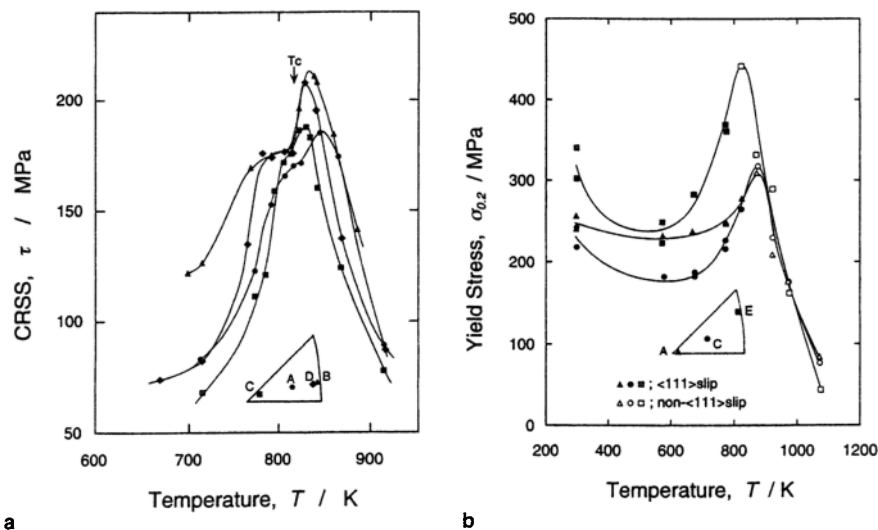


Figure 4. The temperature dependence of yield stress of (a) Fe-25.8Al single crystal in compression and (b) Fe-39.5Al single crystal in compression.

- Mag., 20 (1969), p. 779.
4. T. Yamagata and H. Yoshida, *Mater. Sci. Eng.*, 12 (1973), p. 95.
5. P.A. Flinn, *Trans. Metall. Soc. AIME*, 218 (1960), p. 145.
6. H.J. Leamy and F.X. Kayser, *Phys. Stat. Sol.*, 34 (1969), p. 765.
7. H.J. Leamy, F.X. Kayser, and M.J. Marcinkowski, *Phil. Mag.*, 20 (1969), p. 763.
8. I.L.F. Ray, R.C. Crawford, and D.J.H. Cockayne, *Phil. Mag.*, 21 (1970), p. 1027.
9. R.C. Crawford, I.L.F. Ray, and D.J.H. Cockayne, *Phil. Mag.*, 27 (1973), p. 1.
10. R.C. Crawford and I.L.F. Ray, *Phil. Mag.*, 35 (1977), p. 549.
11. Y. Umakoshi and M. Yamaguchi, *Phil. Mag. A*, 41 (1980), p. 573.
12. Y. Umakoshi and M. Yamaguchi, *Phil. Mag. A*, 44 (1981), p. 711.
13. M.G. Mendiratta, H.-M. Kim, and H. A. Lipsitt, *Metall. Trans. A*, 15 (1984), p. 395.
14. D.G. Morris, D. Peguiron, and M. Nazmy, *Phil. Mag. A*, 71 (1995), p. 441.
15. A. Ball and R.E. Smallman, *Acta Metall.*, 14 (1966), p. 1349.
16. A. Ball and R.E. Smallman, *Acta Metall.*, 14 (1966), p. 1517.
17. M.A. Crimp and Y. Zhang, *High-Temperature Ordered Intermetallic Alloys VI*, vol. 364 (Pittsburgh, PA: MRS, 1995), p. 53.
18. F. Král, P. Schwander, and G. Kostorz, *Acta Mater.*, 45 (1997), p. 675.
19. Y. A. Chang et al., *Intermetallics*, 1 (1993), p. 107.
20. K. Ho and R.A. Dodd, *Scripta Metall.*, 12 (1978), p. 1055.
21. J.P. Neumann, Y. A. Chang, and C.M. Lee, *Acta Metall.*, 24 (1976), p. 593.
22. J.P. Riviere, *Mater. Res. Bull.*, 12 (1977), p. 995.
23. R. Krachler et al., *Intermetallics*, 3 (1995), p. 83.
24. R. Würschum, C. Grupp, and H.E. Schaefer, *Phys. Rev. Lett.*, 75 (1995), p. 97.
25. H.E. Schaefer et al., *Phys. Rev. B*, 41 (1990), p. 11869.
26. D. Paris and P. Lesbats, *J. Nucl. Mater.*, 69&70 (1978), p. 628.
27. C.L. Fu et al., *Phys. Rev. B*, 48 (1993), p. 6712.
28. D. Paris, P. Lesbats, and J. Levy, *Scripta Metall.*, 9 (1975), p. 1373.
29. K. Badura and H.E. Schaefer, *Z. Metallk.*, 84 (1993), p. 405.
30. Y.A. Chang and J.P. Neumann, *Prog. Solid State Chem.*, 14 (1982), p. 221.
31. P. Nagpal and I. Baker, *Met. Trans. A*, 21 (1990), p. 2281.
32. J. Rieu and C. Goux, *Mém. Sci. Rev. Metall.*, 65 (1969), p. 869.
33. D. Weber et al., *J. Phys. C7*, 38 (1977), p. 332.
34. M.A. Crimp and K. Vedula, *Phil. Mag. A*, 63 (1991), p. 559.
35. M.A. Crimp, K.M. Vedula, and D.J. Gaydos, *High-Temperature Ordered Intermetallic Alloys II*, vol. 81 (Pittsburgh, PA: MRS, 1987), p. 499.
36. B. Schmidt, P. Nagpal, and I. Baker, *High-Temperature Ordered Intermetallic Alloys III*, vol. 133 (Pittsburgh, PA: MRS, 1989), p. 755.
37. M.A. Crimp and K.M. Vedula, *Mater. Sci. Eng. A*, 165 (1993), p. 29.
38. K. Yoshimi, Y. Saeki, and S. Hanada, to be submitted.
39. K. Yoshimi, S. Hanada, and M.H. Yoo, *Intermetallics*, 4 (1996), p. 159.
40. J.P. Riviere, H. Zonon, and J. Grilhé, *Phys. Stat. Sol. (a)*, 16 (1973), p. 545.
41. K. Yoshimi et al., *Phil. Mag. A*, 73 (1996), p. 443.
42. N. Junqua, J.C. Desoyer, and P. Moine, *Phys. Stat. Sol. (a)*, 18 (1973), p. 387.
43. A. Fourdeux and P. Lesbats, *Phil. Mag. A*, 45 (1982), p. 81.
44. D.G. Morris, J.C. Loye, and M. Leboeuf, *Phil. Mag. A*, 69 (1994), p. 961.
45. P.R. Munroe, *Intermetallics*, 4 (1996), p. 5.
46. K. Yoshimi and S. Hanada, unpublished work.
47. C.T. Liu, C.G. McKamey, and E.H. Lee, *Scripta Metall. Mater.*, 24 (1990), p. 385.
48. N.S. Stoloff and C.T. Liu, *Intermetallics*, 2 (1994), p. 75.
49. C.G. McKamey, J.A. Horton, and C.T. Liu, *Scripta Metall.*, 22 (1988), p. 1679.
50. C.G. McKamey, J.A. Horton, and C.T. Liu, *J. Mater. Res.*, 4 (1989), p. 1156.
51. C.T. Liu and E.P. Liu, *High-Temperature Ordered Intermetallic Alloys IV*, vol. 213 (Pittsburgh, PA: MRS, 1991), p. 527.
52. P. Nagpal and I. Baker, *Scripta Metall. Mater.*, 25 (1991), p. 2577.
53. M.V. Nathal and C.T. Liu, *Intermetallics*, 3 (1995), p. 77.
54. C.H. Kong and P.R. Munroe, *Processing, Properties, and Applications of Iron Aluminides*, ed. J.H. Schneibel and M.A. Crimp (Warrendale, PA: TMS, 1994), p. 231.
55. C.H. Kong and P.R. Munroe, *Scripta Metall. Mater.*, 30 (1994), p. 1079.
56. J.H. Schneibel et al., *High-Temperature Ordered Intermetallic Alloys VI*, vol. 364 (Pittsburgh, PA: MRS, 1995), p. 73.
57. D.G. Morris, M.M. Dadras, and M.A. Morris, *Acta Metall. Mater.*, 41 (1993), p. 97.
58. M.G. Mendiratta et al., *Metall. Trans. A*, 18 (1987), p. 283.
59. D.J. Gaydos et al., *Mater. Sci. Eng. A*, 150 (1992), p. 7.
60. K. Yoshimi, H. Terashima, and S. Hanada, *Mater. Sci. Eng. A*, 194 (1995), p. 53.
61. N.S. Stoloff and R.G. Davies, *Prog. Mater. Sci.*, 13 (1966), p. 1.
62. I. Baker and P. Nagpal, *Structural Intermetallics*, ed. R. Darolia et al. (Warrendale, PA: TMS, 1993), p. 463.
63. N.S. Stoloff and R.G. Davies, *Acta Metall.*, 12 (1964), p. 473.
64. K. Yoshimi, S. Hanada, and H. Tokuno, *Mater. Trans., JIM*, 35 (1994), p. 51.
65. I. Baker and D.J. Gaydos, *Mater. Sci. Eng.*, 96 (1987), p. 147.
66. J. Guo et al., *Acta Metall. Sinica*, 3 (1990), p. 249.
67. K.-M. Chang, *Met. Trans. A*, 21 (1990), p. 3027.
68. S. Hanada et al., *Scripta Metall.*, 15 (1981), p. 1345.
69. K. Yoshimi, S. Hanada, and M.H. Yoo, *Acta Metall. Mater.*, 43 (1995), 4141.
70. G. Inden and W. Pepperhoff, *Z. Metallk.*, 81 (1990), p. 770.
71. H. Xiao and I. Baker, *Scripta Metall. Mater.*, 28 (1993), p. 1411.
72. J.T. Guo et al., *Scripta Metall. Mater.*, 29 (1993), p. 783.
73. O. Klein and I. Baker, *Scripta Metall. Mater.*, 30 (1994), p. 1413.
74. T. Onuma, M.S. thesis, Tohoku University (1995).
75. N. Matsumoto, M.S. thesis, Tohoku University (1994).
76. R. Carleton, E.P. George, and R.H. Zee, *Intermetallics*, 3 (1995), p. 433.
77. P. Morgand, P. Mouturat, and G. Sainfort, *Acta Metall.*, 16 (1968), p. 867.
78. W. Schröer, H. Mecking, and Ch. Hartig, *Intermetallic Compounds*, ed. O. Izumi (Sendai, Japan: JIM, 1991), p. 567.
79. J.W. Park, I.G. Moo, and J. Yu, *J. Mater. Sci.*, 26 (1991), p. 3062.
80. H. Rösner et al., *Mater. Sci. Eng. A*, 192/193 (1995), p. 793.
81. C.G. McKamey and J.A. Horton, *Met. Trans. A*, 20 (1989), p. 751.
82. K. Yoshimi, S. Hanada, and M.H. Yoo, *High-Temperature Ordered Intermetallic Alloys VII* (Pittsburgh, PA: MRS 1997), in press.
83. R.S. Diehm and D.E. Mikkola, *High-Temperature Ordered Intermetallic Alloys II*, vol. 81 (Pittsburgh, PA: MRS, 1987), p. 329.
84. D.G. Morris, *Phil. Mag. A*, 71 (1995), p. 1281.
85. K. Yoshimi, Ph.D. thesis, Tohoku University (1997).
86. E.P. George and I. Baker, submitted to *Phil. Mag. A*.
87. W. Köster and T. Gödecke, *Z. Metallk.*, 71 (1980), p. 765.

#### ABOUT THE AUTHORS

**Kyosuke Yoshimi** earned his Ph.D. in materials science and engineering at Tohoku University in 1997. He is currently a research associate at Tohoku University.

**Shuji Hanada** earned his Ph.D. in materials science and engineering at Tohoku University. He is currently a professor at Tohoku University. Dr. Hanada is also a member of TMS.

For more information, contact K. Yoshimi at [yoshimi@imr.tohoku.ac.jp](mailto:yoshimi@imr.tohoku.ac.jp).



## San Antonio The 127th TMS Annual Meeting & Exhibition Symposium on Extraction, Refining, and Recycling of LITHIUM

February 15-19, 1998 • Henry B. Gonzalez Convention Center • San Antonio, Texas

This symposium, sponsored by the Reactive Metals Committee of the Light Metals Division of TMS, is designed to promote the understanding of the state of the art in extraction and processing of lithium and its alloys and compounds.

Specific topics to be covered include:

- Extraction and Refining of Lithium Metal: Science, Technology, and Economics
- Lithium Compounds: Synthesis, Properties, and Economics
- Alloys Containing Lithium: Design, Properties, and Economics
- Emerging Markets: Technical Requirements, Economics, Recycling, and Environmental Issues

Any individual involved in lithium or reactive metals research, processing, or application is encouraged to attend this symposium.

The 1998 TMS Annual Meeting & Exhibition will attract more than 3,800 of your colleagues to San Antonio for more than 1,000 presentations addressing all aspects of materials science and metallurgical engineering. In addition, special lectures, tutorials, social events, and a 25,000 square-foot exhibit by the world's top providers of technology, materials, and services are scheduled. Don't miss it.

For more information on the Symposium on Extraction, Refining & Recycling of Lithium or the 1998 TMS Annual Meeting & Exhibition, please contact:

TMS Customer Service  
420 Commonwealth Drive  
Warrendale, PA 15086-7514

Telephone: 1-800-759-4867 or (412) 776-9000, ext. 270

Fax: (412) 776-3770

E-mail: [csc@tms.org](mailto:csc@tms.org)

**TMS**  
Minerals • Metals • Materials

or

Visit the TMS Annual Meeting & Exhibition home page on the World Wide Web at <http://www.tms.org/Meetings/TMS-Annual-Meetings.html> for complete up-to-the-minute information.